

Original Article

Cite this article: Wen H, Xu W, Li Y, You Y, and Luo X (2020) Siliceous-sulphate rock coatings at Zhenzhu Spring, Tengchong, China: the integrated product of acid-fog deposition, spring water capillary action, and dissolution. *Geological Magazine* **157**: 201–212. <https://doi.org/10.1017/S0016756819000542>

Received: 6 June 2018

Revised: 14 April 2019

Accepted: 26 April 2019

First published online: 6 June 2019

Keywords:

gypsum; amorphous silica; rock coating; hot spring; Tengchong

Author for correspondence: Huaguo Wen and Wenli Xu, Emails: wenuhuaguo08@cdu.cn and xuwenli5@163.com

Siliceous-sulphate rock coatings at Zhenzhu Spring, Tengchong, China: the integrated product of acid-fog deposition, spring water capillary action, and dissolution

Huaguo Wen^{1,2,*} , Wenli Xu^{1,2,*}, Yi Li², Yaxian You² and Xiaotong Luo²

¹State Key Laboratory of Oil and Gas Reservoir Geology and Exploitation, Chengdu University of Technology, Chengdu 610059, China and ²Institute of Sedimentary Geology, Chengdu University of Technology, Chengdu 610059, China

Abstract

Siliceous-sulphate rock coatings were observed at Zhenzhu Spring, an acid sulphate hot spring in the Tengchong volcanic field, China. These rock coatings are mainly formed of gypsum and amorphous silica. Some alum-(K), voltaite, α -quartz and muscovite were also found. Four different laminae are developed in the rock coatings: gypsum layer, tight siliceous layer, tabular siliceous layer and siliceous debris layer. The gypsum layer is located at the top of the rock coatings, while other siliceous layers appear below the gypsum layer. Geochemical modelling of the fluids was performed to identify the mechanisms responsible for the formation of gypsum and amorphous silica. The results indicated that the occurrence of gypsum is related to the acid-fog deposition and amorphous silica mainly originates from spring water. Fog deposition provided the rock coatings with abundant SO_4^{2-} and Ca, and the subsequent complete evaporation of the condensed fluids produced gypsum. Seasonal climate change (especially variation in rainfall) determines the fluctuations of capillary action and dissolution. Rainfall events in the wet season led to periods of non-precipitating gypsum and promoted the capillary rise of the spring water. Slightly diluted capillary water (a small amount of rainwater) covered the rock coatings, formed a tight siliceous layer on the rock-coating surface and/or filled the pores among the gypsum crystals forming many tabular siliceous aggregates. Heavy rainfall (high dilution), however, resulted in non-precipitating amorphous silica and accelerated the gypsum dissolution, leaving tabular pores around tabular siliceous aggregates and forming a tabular siliceous layer.

1. Introduction

Volcanic and/or geothermal fields throughout the world are common sites that develop silica (e.g. amorphous silica) and sulphate minerals (e.g. gypsum). Although these silica and sulphate minerals can be precipitated in subaqueous environments, such as hot springs and crater lakes (e.g. Pierre & Alain, 1994; Peng & Jones, 2012; Tang *et al.* 2014), some of them were also found in many subaerial environments, such as volcanic fumaroles and soils around geysers (Ciesielczuk *et al.* 2013; Hynek *et al.* 2013; Piochi *et al.* 2015). Some silica and/or sulphate minerals are present as rock coatings in volcanic and/or geothermal fields (Schiffman *et al.* 2006; Minitti *et al.* 2007; Yant *et al.* 2018), with different compositions compared to their underlying rocks. The formation of silica and/or sulphate rock coatings is complex and scientists have suggested various explanations, such as acid-fog deposition, vapour deposition and condensate-rock interaction (e.g. Kodosky & Keskinen, 1990; Africano & Bernard, 2000; Schiffman *et al.* 2006; Aguilera *et al.* 2016; Rodríguez & van Bergen, 2016).

Acid fog (acid aerosol) in volcanic fields is generally thought to be the product of sulphurous gases (SO_2 and H_2S) emitted from volcanoes (Settle, 1979; McCanta *et al.* 2014). Acid fog is also present above acid sulphate-rich hot water pools (Rodgers *et al.* 2000; Bogdan *et al.* 2013), largely due to the gas release (mainly H_2S) at the pool bottom and fast evaporation and subsequent condensation of hot water. Acid-fog deposition on the rock surface may form silica and/or sulphate minerals because of the fluid-rock interaction (Tosca *et al.* 2004; Schiffman *et al.* 2006). Capillary action of spring water is ubiquitous around hot springs and geysers, and is considered to be a significant factor that accelerates the accumulation of subaerial silica and/or sulphate minerals (Renaut *et al.* 1998; Jones & Renaut, 2006; Ciesielczuk *et al.* 2013). Dissolution of sulphate minerals, especially soluble metal sulphate minerals, can influence their preservation and distribution (Valente & Gomes, 2009), mainly because of the high solubility that allows them to be easily dissolved in meteoric water (e.g. rainstorm).

Zhenzhu Spring in the Rehai geothermal field develops rock coatings around the pool wall. These rock coatings are continuously in contact with the fog arising from the pool surface and

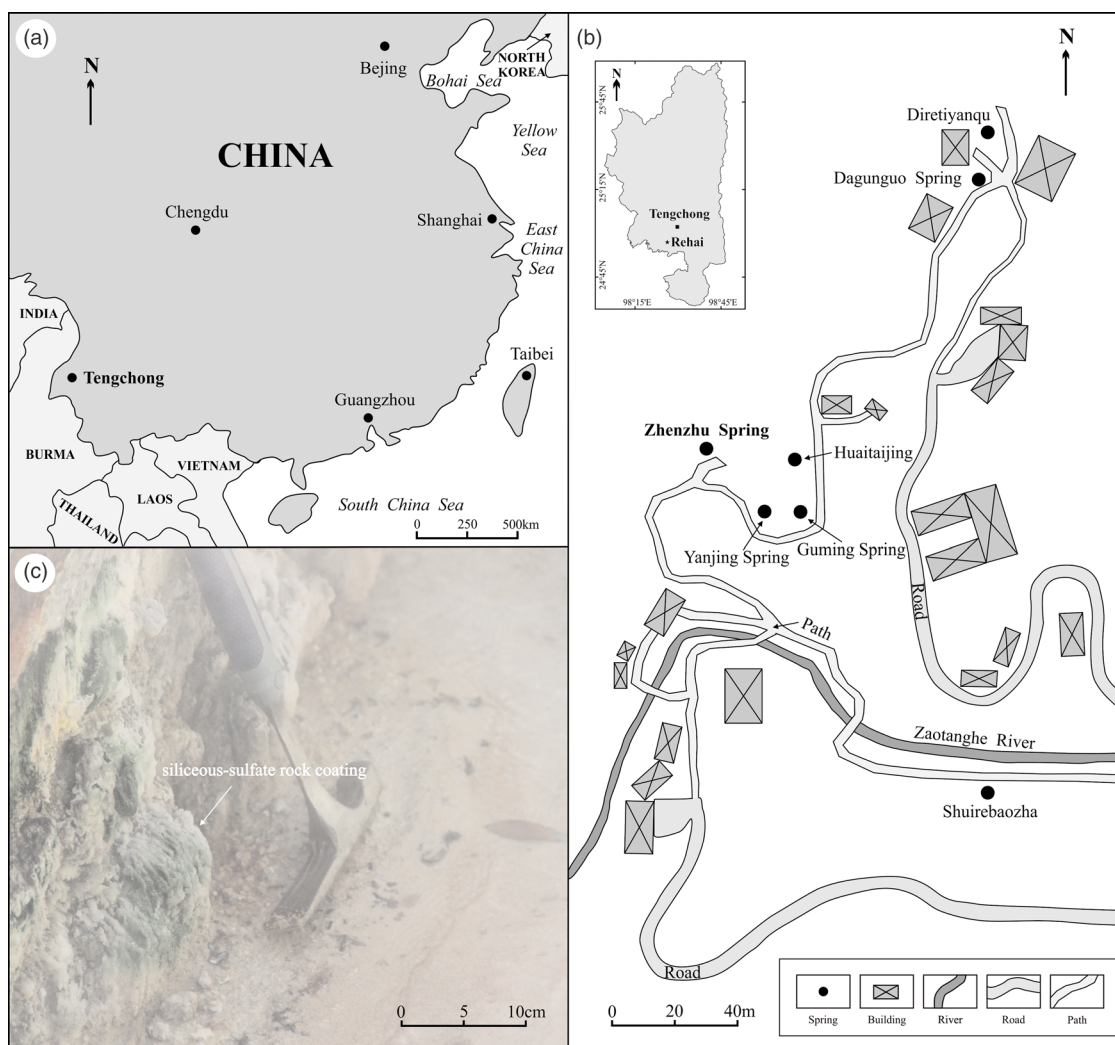


Fig. 1. (Colour online) Location of (a) Tengchong in SW China and (b) the Rehai geothermal field, Tengchong, showing the locations of Zhenzhu Spring and other springs (Guming Spring, Yanjing Spring, etc.). (c) Siliceous rock coatings at Zhenzhu Spring.

are located in areas where the capillary action of the spring water may develop. These siliceous-sulphate coatings experience high rainfall in the wet season that could modify the development of sulphate minerals. To evaluate the effect of fog deposition, spring water capillary action, and dissolution, on the development of the rock coatings at Zhenzhu Spring, we report (1) the fluid (spring water and condensed fluid) chemistry, (2) the mineralogical composition of the rock coatings, (3) the different laminae of the rock coatings and (4) the fluid cooling, evaporation and dilution and the reaction path models of water–rock interactions. Integration of this information shows that the impact of fog deposition in acid sulphate hot springs on the formation of subaerial sulphate minerals is notable. In addition, this study demonstrates that the capillary action of the spring water may cause the precipitation of subaerial amorphous silica. Additionally, rainfall events could, to some extent, control the capillary action of the spring water and the dissolution of some sulphate minerals around hot springs.

2. General setting

The Rehai geothermal field is located in the southern part of the Tengchong volcanic field, c. 11 km from Tengchong City

(Fig. 1a, b). One magma body with an average temperature of more than 560 °C (Zhao *et al.* 2011), a depth of 5–6 km, and a thickness of 15–20 km, underlies the study area (Bai *et al.* 2001). Influenced by the residual heat from the magma chamber, the Rehai geothermal field develops many strong geothermal manifestations: hydrothermal explosions, fumaroles, steaming ground, hydrothermal alteration, hot springs, siliceous sinters and hot-spring travertines (e.g. Shangguan *et al.* 2005; Guo & Wang, 2012; Jones & Peng, 2015; Luo *et al.* 2019a, b). Numerous hot springs (42–96 °C) (Guo, 2012) occur in the valley of the Zaozanghe River (Fig. 1b). These hot spring fluids are largely derived from meteoritic waters (Du *et al.* 2005; Zhang *et al.* 2008; Guo, 2012). Moreover, water–rock interactions and/or the mixing between magmatic fluids and meteoric waters cause different changes in fluid composition (Du *et al.* 2005; Zhang *et al.* 2016b). The temperature values of the geothermal reservoirs (Proterozoic metamorphic rocks and Yanshanian granites) (Guo & Wang, 2012) are mainly in the range 200–250 °C (Shangguan, 2000). Tengchong County, which includes the Rehai geothermal field, is characterized by a highland subtropical climate and can be divided into wet season (May to September) and dry season (October to April) (Jones & Peng, 2015).

Zhenzhu Spring (also known as Pearl Spring, Zhenzhuquan, or Zhenzhuquan Spring), with Na–SO₄–Cl type waters, is a special steam-heated hot spring in the Rehai geothermal field (Zhang *et al.* 2016b). The characteristics of Zhenzhu Spring include (1) high-temperature (84.3–96 °C), low-pH (generally ≤4.5) spring waters (Zhang *et al.* 2008, 2016b; Guo & Wang, 2012; Guo *et al.* 2014; Jiang *et al.* 2018), (2) high CO₂ (88.7–84.5 %) and low N₂ (1.7–7.98 %), O₂ (0.03–2.77 %), Ar (0.004–0.13 %), H₂ (5 %), CH₄ (0.03–0.05 %) and H₂S (0.11–0.28 %) contents (Shangguan *et al.* 2000; Zhang *et al.* 2016a), (3) abundant fog above the water surface due to boiling and bubble bursting, (4) deposits of various detrital lithic grains and no amorphous silica in the pool bottom, and (5) rock coatings developed around the pool (Fig. 1c). Previous studies (e.g. Zhang *et al.* 2008; Guo & Wang, 2012) have shown that the acidic waters from Zhenzhu Spring contain higher concentrations of SO₄²⁻ and SiO₂ than most alkaline hot springs (predominant ions: Cl⁻, HCO₃⁻, Na and SiO₂) in the Rehai geothermal field. Low pH values and the enrichment of SO₄²⁻ in the acidic spring waters may be formed by separation of vapours rich in H₂S from the reservoirs and subsequent condensation and oxidization in shallow oxygen-rich groundwater or surface water (Guo & Wang, 2012; Jiang *et al.* 2018), while the intense water–rock interactions in underground reservoirs result in the presence of large amounts of SiO₂ (Zhang *et al.* 2008).

3. Methods

Field observations and sampling at Zhenzhu Spring were conducted in January 2018. One sample was filtered through a 0.45 µm cellulose acetate filter. For SiO₂ analysis, the spring water was diluted tenfold with deionized water to prevent the precipitation of SiO₂. Water samples for cation analysis were acidified (pH ≤ 1) with a few drops of concentrated HNO₃ and analysed with ICP-AES (iCAP 6000 Series, Thermo Scientific), which was also used to analyse the SiO₂ concentrations. The CO₃²⁻ and HCO₃⁻ concentrations of unacidified water samples were determined by the titration method (Jackson, 1958), while the Cl⁻ and SO₄²⁻ concentrations were measured using ion chromatography (Dionex ICS 5000+, Thermo Scientific).

Only those rock coating samples developed at a location that the spring water can reach by capillary action, and their underlying rocks were used in this study. Fourteen samples were powdered using a mortar and pestle and were sent for mineralogical identification by X-ray diffraction (XRD) analysis utilizing a Cu–Kα radiation with a step of 0.02° and 2θ range of 5–60° (DX-2700, Dandong Haoyuan). We extracted 19 small fractured samples (~1 cm³) from the large samples and coated them with gold. After these preparation steps, small fractured samples were examined on a QUANTA 250 FEG-scanning electron microscope (SEM) at 5 kV to observe mineral crystal morphology. Furthermore, detailed energy-dispersive X-ray (EDX) analyses were performed with an accelerating voltage of 20 kV and an average beam spot size of 1 µm (Oxford INCAx-max20 X-ray spectrometer) in order to identify the mineral elemental composition.

PHREEQC software, Version 2.5 (Parkhurst & Appelo, 1999), was employed to simulate the cooling, evaporation and dilution processes of the fluids, and the reaction path of water–rock interactions. We chose the Lawrence Livermore National Laboratories thermodynamic database (llnl.dat) for the simulations. All models were started with 1 kg of fluid. In view of the simple mineral composition of the rock coatings from Zhenzhu Spring, only representative minerals (gypsum and amorphous silica) were selected to

precipitate during each run. Since the siliceous-sulphate rock coatings at Zhenzhu Spring develop in a surficial environment, we selected a low temperature range (5–95 °C) to simulate the processes possibly occurring at Zhenzhu Spring.

The cooling modelling was conducted at temperatures from 95 °C (about the highest water temperature of Zhenzhu Spring) to 5 °C (close to the lowest air annual temperature in Tengchong) (Jones & Peng, 2015). For fluid evaporation simulations, three temperature values were used, including 90 °C (approximately the spring water temperature) representing an uncooled fluid, 20 °C (close to the ambient temperature) representing a fully cooled fluid, and 55 °C representing a partially cooled fluid. Pure water with no ions was continuously added into the fluids to model the changes in the saturation states of minerals during the dilution processes. Although the mineral saturation index (SI) can reflect the precipitation tendency of various minerals, the simulation processes in this study do not consider the effect of reaction kinetics and always assume thermodynamic equilibrium. Water–rock reaction models were built using the same method used by Rodríguez & van Bergen (2017): 1 mol of the underlying rocks was reacted with 1 kg of the fluids (spring water, condensed fluid). Moreover, the simulations of water–rock interaction assumed that no quartz was dissolved in the fluids because of the low dissolution rate of quartz in acid fluids (Henderson *et al.* 1970; Knauss & Wolery, 1988).

4. Results

4.a. Fluid chemistry

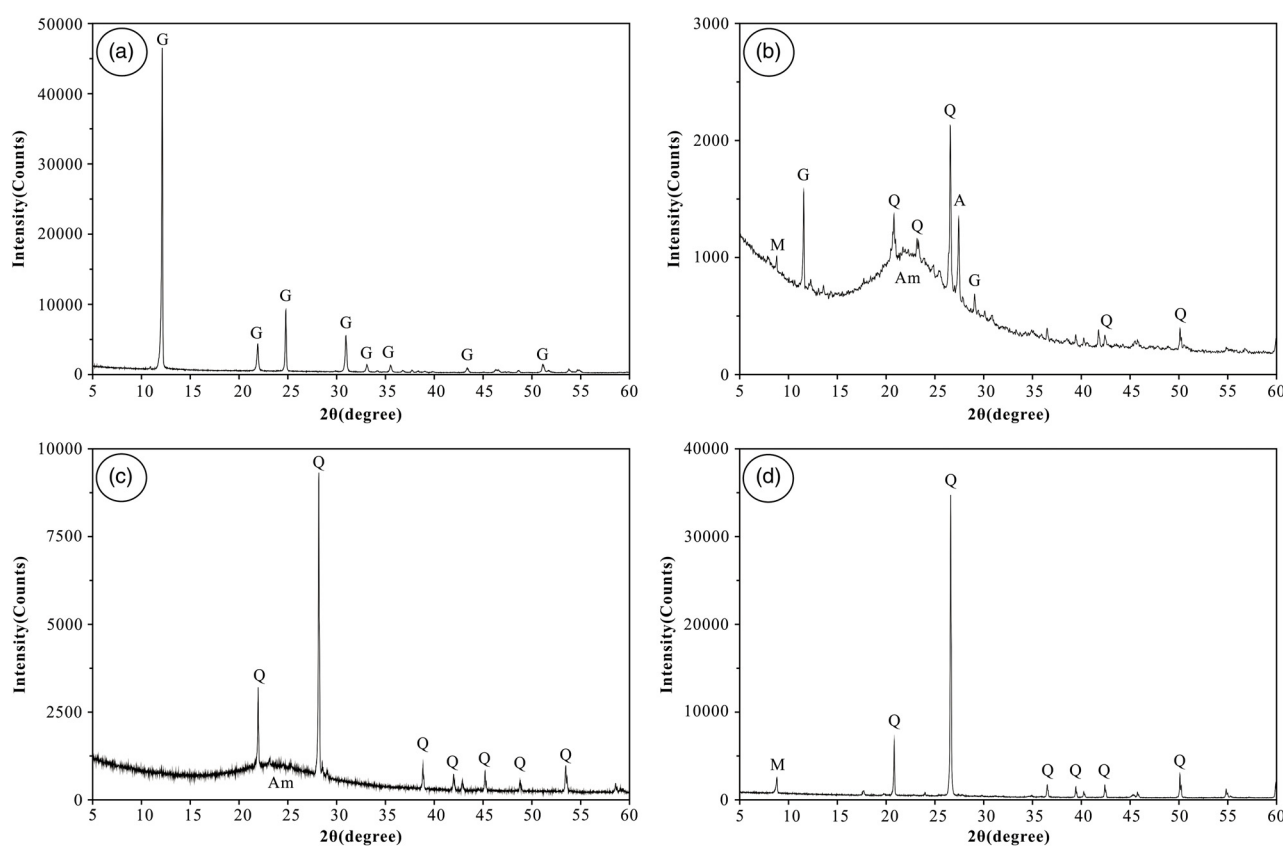
Fluid characteristics in this study and the previous studies are listed in Table 1. The results show no significant differences in temperature (*c.* 90 °C) and concentrations of most ions (except for SiO₂). The spring waters are deficient in HCO₃⁻, Mg, Al and Ca, and rich in Cl, SO₄²⁻, Na, K and SiO₂ (Table 1). With respect to pH and SiO₂, Guo & Wang (2012) report a near-neutral pH (6.42) and a higher SiO₂ concentration (262 mg L⁻¹), while other studies describe lower pH values (≤4.5) and SiO₂ concentrations (<160 mg L⁻¹). Comparison of the results with those of other studies also reveals some differences in Na, Cl⁻, SO₄²⁻ and HCO₃⁻. Although the reasons for these contrasts are not clear, they might be: (1) analytical problems in ion analysis, and (2) temporary changes in composition of spring waters. Cations detected in the acid condensed fluid from Zhenzhu Spring include Ca, Na, Mg and K, while anions contain SO₄²⁻ and Cl (Table 1). A distinct enrichment of SO₄²⁻ and Ca was observed in the condensed fluid from Zhenzhu Spring. Although the spring waters and the condensed fluid are different in fluid composition, they have a similar abundance of SO₄²⁻.

4.b. Mineralogy

XRD analyses (Fig. 2) and SEM analyses (Fig. 3) show the simple mineral composition of the rock coatings and the underlying rocks from Zhenzhu Spring. The former are composed of gypsum, amorphous silica, alum-(K) [KAl(SO₄)₂·12H₂O], α-quartz and muscovite (Fig. 2a–c), while the latter which might be derived from the alteration of silicified fractured syenogranites (Lin *et al.* 2014) in the Rehai geothermal field are represented by α-quartz and muscovite (Fig. 2d). A small number of granular angular sulphate minerals (Fig. 3h) were also observed in the SEM analysis, but their contents were too low to be checked in the XRD spectrums. In this study, these sulphate minerals are identified as voltaite [K₂Fe²⁺₅Fe³⁺₃Al(SO₄)₁₂·18H₂O], based on repetitive EDX

Table 1. Chemical analyses of water samples from Zhenzhu Spring in the Rehai geothermal field (concentration in mg L⁻¹, blank = no data, ND = not detected, * = measured in the lab)

Reference	Fluid	T (°C)	pH	K	Na	Ca	Mg	Al	Fe	Cl	SO ₄ ²⁻	HCO ₃	SiO ₂
Zhang <i>et al.</i> (2008)	Spring water	96	3.5	13.7	13	1.71	0.04		0.204	38.1	134	ND	153
Guo & Wang (2012)	Spring water	96	6.42	15.9	67.7	2.3	0.4			39.2	128.2	5.6	262
Guo <i>et al.</i> (2014)	Spring water	91.8	4.5	21.7	58.5	2.16	0.61	0.46	1.33	64.3	162	12.8	140
Jiang <i>et al.</i> (2018)	Spring water	88.50	3.93	22.30	51.37	3.13	0.47	0.35	0.56	40.30	115.73	16.30	
Luo <i>et al.</i> (2019b)	Condensed fluid	19.6*	3.22*	0.183	0.267	5.11	0.185	ND	ND	0.107	34	ND	0.295
This research	Spring water	89.5	4.50*	22.9	30.8	2.49	0.548	0.739	0.572	46.4	98.9	28.46	126

**Fig. 2.** Representative X-ray diffraction patterns of the rock coatings and their underlying rocks at Zhenzhu Spring. G = gypsum, Am = amorphous silica (a ‘hump’ shape), A = alum-(K), Q = α -quartz, M = muscovite. (a) Newly formed gypsum sampled from the surficial rock coatings. (b, c) Previously formed minerals sampled from the lower part (close to the underlying rock) of rock coatings. (d) Abundant α -quartz and some muscovite constitute the underlying rocks.

analyses which show that they are mainly composed of K, Fe, Al, S, O. Since α -quartz and muscovite might be derived from the underlying rocks or soils, this study predominantly focuses on the rest of the minerals, which may be formed either by fog deposition, spring water capillary action or the alteration of underlying rocks.

Gypsum is the most abundant sulphate mineral and mainly occurs at the top of the rock coatings at Zhenzhu Spring. Two types are recognized: tabular (Fig. 3a) and prismatic (Fig. 3b, c). Tabular gypsum crystals are common in the rock coatings and are characterized by long crystals (≥ 0.5 mm). Some less common prismatic gypsum crystals also appear and can be divided into large (≥ 100 μ m) (Fig. 3b) and small crystals (≤ 100 μ m) (Fig. 3c). In this study,

apart from a few gypsum crystals found to be embedded in amorphous silica (Fig. 3d), most of the gypsum crystals were present above the amorphous silica (Fig. 3a).

Amorphous silica typically appears in the lower part of the rock coatings at Zhenzhu Spring and varies in occurrence. This mineral is apparent in the XRD spectra (Fig. 2b, c) with a broad hump centred around 21.9° (2θ) (Herdianita *et al.* 2000). Amorphous silica is found as: (1) a coating on the surfaces of the gypsum crystals (Fig. 3e), (2) tabular aggregates made of granular amorphous silica (Fig. 3f), (3) amorphous silica debris likely formed by the breakage of tabular amorphous silica aggregates (Fig. 4) and (4) tight layers with some pores developed in them (Fig. 3g). Some alum-(K)

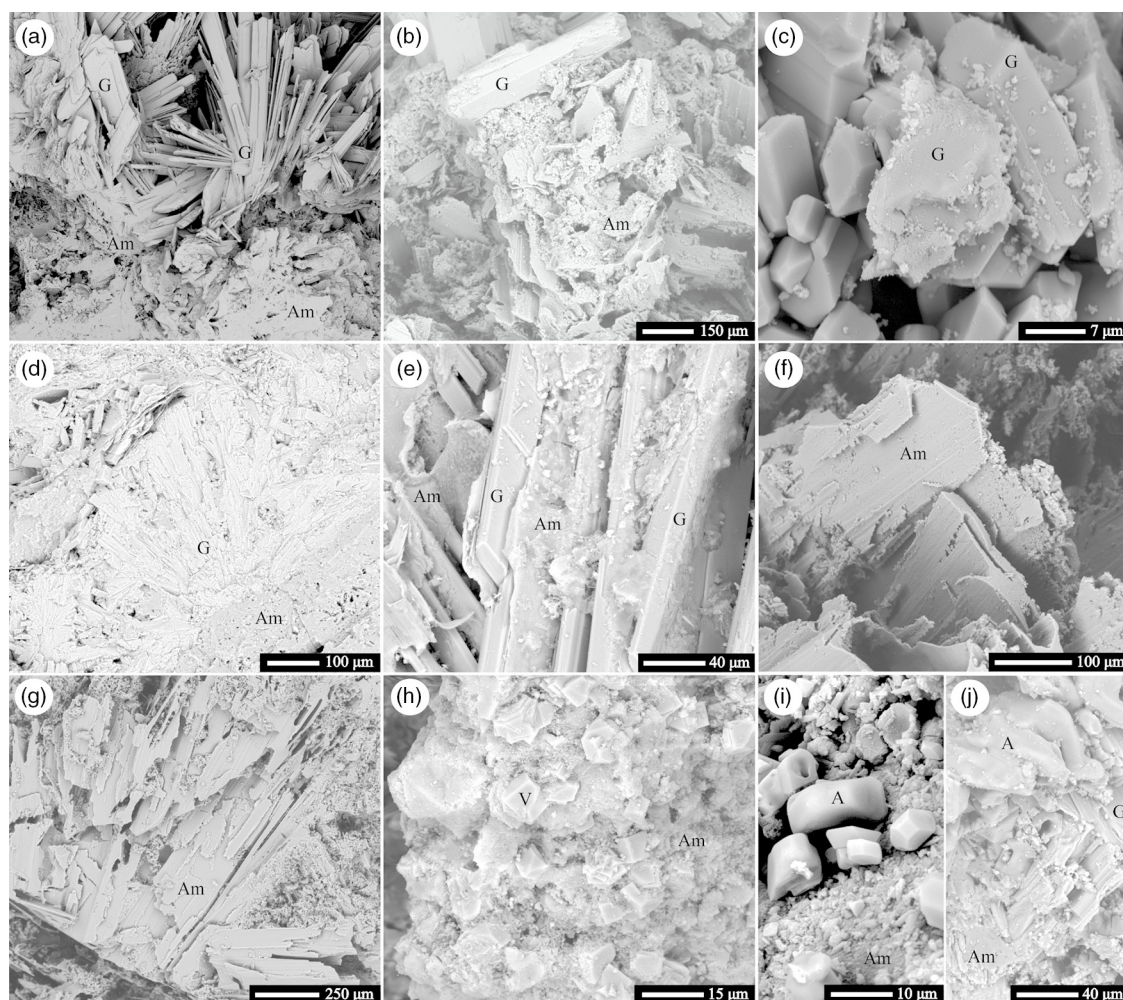


Fig. 3. Backscattered electron photographs of gypsum crystals, amorphous silica, voltaite and alum-(K). G = gypsum, Am = amorphous silica, V = voltaite, A = alum-(K). (a) Tabular gypsum crystals develop on amorphous silica. (b) Large prismatic gypsum crystals and amorphous silica aggregates. (c) Small prismatic gypsum crystals. (d) Tabular gypsum crystals (light parts) embedded within amorphous silica (dark parts). (e) Amorphous silica coating present on gypsum crystal surfaces. (f, g) Tabular amorphous silica aggregates. (h–j) voltaite alum-(K) in the sulphate rock coatings.

and trace voltaite were found in some samples (Figs 2b, 3h–j), commonly in association with amorphous silica.

4.c. Laminae

Most of the rock coatings at Zhenzhu Spring are laminated, with the layers varying in mineral composition and/or occurrence (Fig. 4). Four different layers were observed, including the gypsum layer formed of tabular or prismatic gypsum crystals, the tabular siliceous layer composed of tabular amorphous silica aggregates, the siliceous debris layer characterized by amorphous silica debris, and the tight siliceous layer. The gypsum layer developed at the top of the rock coatings, whereas other layers appeared below the gypsum layer (Fig. 4). The lower part of the rock coatings at Zhenzhu Spring is formed of alternating tight siliceous layers and tabular siliceous layers (or siliceous debris layers). Although three types of siliceous layers exist in some rock coating samples at Zhenzhu Spring (Fig. 4b), there may be only two types of layers because of the high probability that the siliceous debris layers are the result of the breakage (and dissolution) of tabular siliceous layers.

4.d. Geochemical modelling

The cooling model of the condensed fluid from Zhenzhu Spring shows that the condensed fluid was unsaturated with gypsum and amorphous silica (Fig. 5a). A temperature fall can increase the SI value of amorphous silica and cause a subtle decrease in pH and the SI value of gypsum (Fig. 5a). The temperature changes will not drive the condensed fluid to precipitate any mineral because of their low SI values (<0). The evaporation of the condensed fluid will account for the rapid rise of SI and the decrease in pH, especially during the last stage of evaporation ($H_2O > 80\%$) (Fig. 5b). Such a pH decrease would cause the waters to become more acidic. Acid fluids are generally not favourable to gypsum precipitation due to sulphuric acid equilibrium (i.e. forming more $H_2SO_4^-$ and improving the solubility of gypsum), but the SI_{gypsum} values still increase during the evaporation processes (Fig. 5b). This shows that the pH increase of the condensed fluid plays a secondary role in the formation of gypsum during the evaporation processes. The complete evaporation of the condensed fluid is necessary for gypsum and amorphous silica formation. Compared with other cations, anions and dissolved SiO_2 in the condensed fluid (Table 1), its relatively high concentrations of Ca and SO_4^{2-} in the condensed

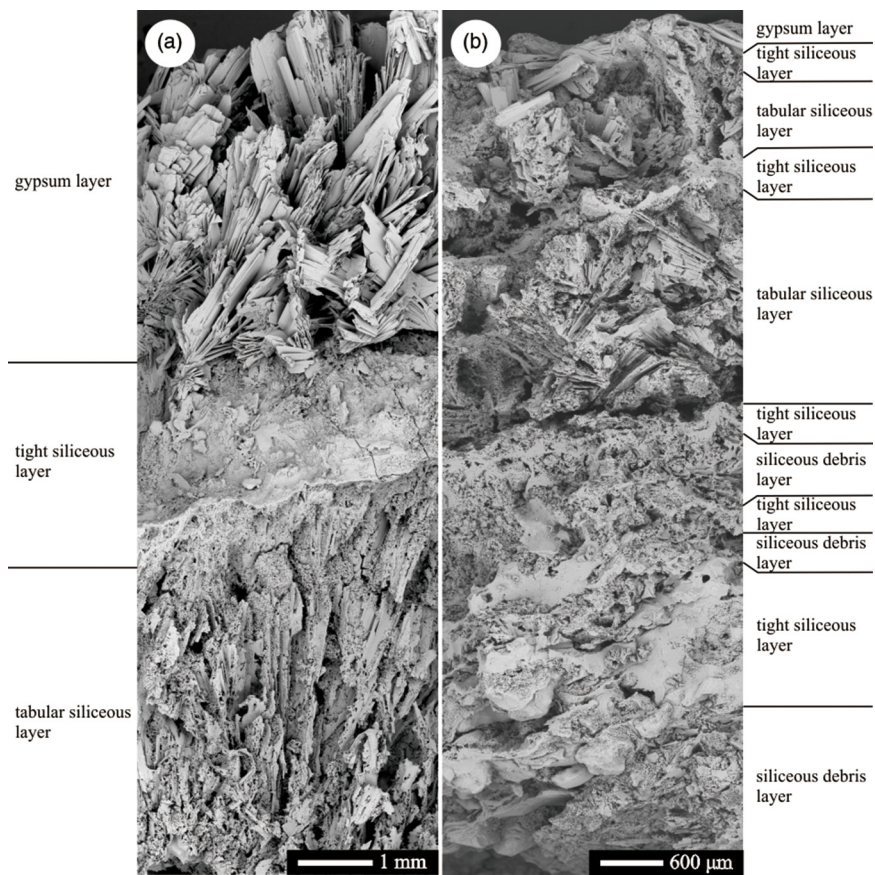


Fig. 4. Backscattered electron photographs of different laminae.

fluid show that the most abundant mineral produced during the evaporation of the condensed fluid is gypsum instead of amorphous silica.

With the cooling of the spring water from Zhenzhu Spring, the SI value of amorphous silica increases, while the SI value of gypsum decreases (Fig. 5c). The change in the SI value of gypsum was subtle. Compared with the SI values of gypsum, the changes in the SI values of amorphous silica are relatively large and may cause the precipitation of amorphous silica when the spring water cools down to 30 °C. Unless the spring water is completely evaporated, no gypsum can be precipitated (Fig. 5d). The precipitation of amorphous silica is influenced not only by temperature (Fig. 5c), but also by the percentage of H₂O evaporated (Fig. 5d). A larger proportion of H₂O evaporated and a lower temperature will promote the precipitation of amorphous silica (Fig. 5c, d). For instance, the SI value of amorphous silica will steadily increase during the spring water evaporation at 90 °C until c. 66 % of the water is evaporated and then the amorphous silica will be precipitated (Fig. 5d). However, if the spring water is evaporated at 20 °C, the amorphous silica will be formed even if no spring water evaporation occurs because of its high SI values (>0) (Fig. 5d).

A precipitation–dissolution model (Fig. 5e) and a dilution model (Fig. 5f) were run in PHREEQC to estimate the variations in the amounts of amorphous silica precipitation and dissolved gypsum in the spring water at different temperatures, and the saturation states of the minerals in the mixed fluid of spring water

with meteoric water (pure water). The curve of gypsum is near horizontal (Fig. 5e), which shows the temperature changes have little influence on the gypsum dissolution amount. Amorphous silica precipitation would start at c. 30 °C (Fig. 5c, e) when the SI values of amorphous silica arrive at 0. Unlike the near-constant dissolution amount of gypsum (Fig. 5e), a lower temperature would lead to more amorphous silica precipitates (Fig. 5e) largely because of the continuous and rapid rise of SI of amorphous silica during cooling processes (e.g. Hinman & Lindstrom, 1996; Guidry & Chafetz, 2002). The dilution model suggests that dilution facilitates the dissolution of gypsum and slows down the precipitation rate of amorphous silica (Fig. 5f). After 0.35 times pure water was added, amorphous silica became unsaturated in fluids (Fig. 5f).

Figure 5g shows that although spring-water – rock interactions and condensed-fluid – rock interactions cause differences in the number of secondary minerals and in the reaction progress value, both alunite and amorphous silica can be formed. The underlying rocks can release Al and K and form alunite at low–intermediate reaction progress values (<0.1 mol rock / kg water). Unfortunately, no alunite was detected at Zhenzhu Spring, which means that alunite may not be formed or may have been converted to other minerals. In this study, we consider alum-(K) to be the product of transformation (dissolution, evaporation and crystallization) of alunite, as proposed by Singer (1948) and Archontidou *et al.* (2005). Amorphous silica appears at intermediate–high reaction progress values (c. 0.01–1 mol rock / kg water).

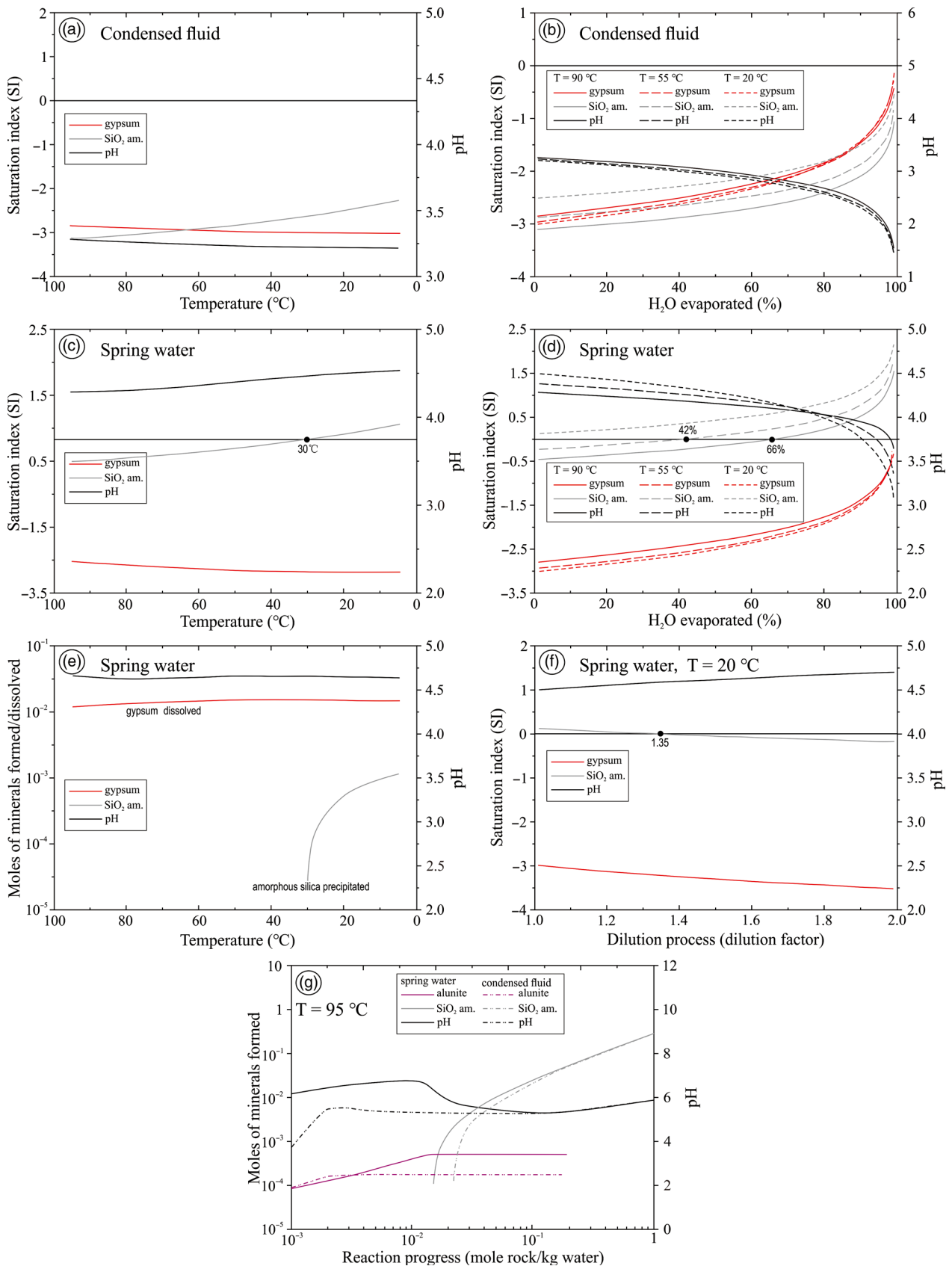


Fig. 5. (Colour online) Geochemical models of the condensed fluid (a, b) and the spring water (c–f) showing the saturation indexes and the number of moles formed/dissolved of minerals. (a) Cooling model of the condensed fluid. (b) Isothermal evaporation model of the condensed fluid. (c) Cooling model of the spring water. (d) Isothermal evaporation models of the spring water. (e) Moles of amorphous silica formed and gypsum dissolved at different temperatures in the undiluted spring water. (f) Dilution model of the spring water. (g) Water–rock reaction path models (spring water versus underlying rock, condensed fluid versus underlying rock).

5. Discussion

5.a. Genesis of sulphate minerals and acid-fog deposition

Interpretations of the genesis of subaerial sulphate minerals in volcanic and geothermal fields are various (e.g. Rodgers *et al.* 2000; Schiffman *et al.* 2006; Hynek *et al.* 2013; Szynekiewicz *et al.* 2014). A rock–fluid (e.g. rock–vapour, rock–condensate) interaction is commonly considered responsible for the development of sulphate minerals at many sites, such as Diana Cave, Romania (Bogdan *et al.* 2013), and active volcanoes in Nicaragua (Hynek *et al.* 2013) and Costa Rica (Poás volcano) (Rodríguez & van Bergen, 2017). However, this mechanism is inapplicable at Zhenzhu Spring because of (1) the stable mineral composition of the underlying rocks (*c.* 90 % α -quartz and 10 % muscovite; Fig. 2d), which can only produce a weak fluid–rock interaction and provide no or little Ca for gypsum, and (2) a small number of aluminium-containing sulphate minerals, indicating that only small amounts of aluminium and potassium were released from the underlying rocks.

The gases from Zhenzhu Spring contain some H₂S (0.11–0.25 %) and SO₂ (0.0051 %) (Shangguan *et al.* 2000; Zhang *et al.* 2016a). Although sulphate minerals formed directly from the sulphur-containing gases (as sublimates) have been found at some volcanic fumaroles (e.g. Kavalieris, 1994; Taran *et al.* 2001; Aguilera *et al.* 2016) and burning coal-dumps (Shimobayashi *et al.* 2011), high gas temperatures (generally >300 °C) are necessary for the formation of these sulphate minerals. At Zhenzhu Spring, vapour deposition cannot cause the occurrence of sulphate minerals because of its low temperatures (at least, vapour deposition is not the main factor controlling the formation of sulphate minerals). Additionally, the evaporation of the capillary spring water can form sulphate minerals in subaerial conditions (Zhu *et al.* 1982; Ciesielczuk *et al.* 2013; Szynekiewicz *et al.* 2014), but the geochemical models of the spring water from Zhenzhu Spring (Fig. 5c, d) show the preferential formation of amorphous silica instead of gypsum.

Precipitation of gypsum from the capillary spring waters requires complete evaporation of the spring waters, possibly because of the low concentrations of Ca in spring waters and the low pH (Table 1). The complete evaporation of the capillary spring waters would form large amounts of saline minerals (e.g. halite) instead of gypsum due to the high contents of Na, K, Cl and SO₄²⁻ in the spring waters (Table 1). However, we found no other saline minerals in the rock coatings, suggesting full evaporation of the capillary waters was never achieved near the rock coatings at Zhenzhu Spring. We thus exclude the possibility that the gypsum in the rock coatings was directly precipitated from capillary waters.

Fog (composed of steam and vapour) can be formed around hot springs (e.g. Rodgers *et al.* 2000; Bogdan *et al.* 2013), possibly by the bubble bursting on the water surface, vapour release from the pool-bottom vents and rapid evaporation of spring waters. The close link between sulphate minerals and fog has been found in deserts (Leybourne *et al.* 2013) and volcanoes (McCanta *et al.* 2014; Yant *et al.* 2018). The fog (condensed fluid) from Zhenzhu Spring contains some ions (Table 1). The acid-fog deposition on the rock surface produced the condensed fluids. After the complete evaporation of these fluids (Fig. 5b), abundant sulphate minerals (mainly gypsum because of the enrichment of Ca and SO₄²⁻, and the rarity of other ions in the condensed fluids) were formed on the rock-coating surface. This fog deposition model can also explain why the gypsum commonly occurred at

the top of the rock coatings from Zhenzhu Spring. It is noticed that some condensed fluids can react with the underlying rocks (mainly muscovite) and cause the occurrence of aluminium-containing sulphate minerals (e.g. alunite) (Fig. 5g). These condensed fluid–rock interactions become stronger with the cooling of condensed fluids due to the decrease of pH (Fig. 5a).

5.b. Origin of silica and capillary action

The rock coatings from Zhenzhu Spring are characterized by the occurrence of amorphous silica below the gypsum crystals (Fig. 4), which partly reflects the presence of SiO₂-containing fluids. In terrestrial hot spring settings, amorphous silica is commonly precipitated from spring waters because of rapid cooling, evaporation, changes in pH, and cation effects (Guidry & Chafetz, 2002; Handley *et al.* 2005; Tobler *et al.* 2008). Spring waters are the main sources of silica for subaqueous amorphous silica precipitates (sinter) in hot springs. In environments (especially in acid-sulphate environment) related to hot springs, surrounding rocks are likely the predominant origin of silica. For example, amorphous silica found on the surface of the geothermal fields in New Zealand was formed as the primary silica residue of the acid-sulphate alteration of volcanic rocks (Rodgers *et al.* 2002, 2004). With respect to silicate minerals, especially feldspar and kaolinite, their long-time presence in the acid-sulphate environment would cause the formation of silica minerals (Martin *et al.* 2000; Kruszewski, 2013).

At Zhenzhu Spring, amorphous silica from the rock coatings was largely issued from the spring water. The underlying rock can produce amorphous silica during water–rock interactions (Fig. 5g). However, their contribution was not important because (1) only a few silicate minerals that may form amorphous silica during acid-sulphate alteration processes were observed in the underlying rocks (Fig. 2d), and (2) only a small amount of alum-(K) was detected, indicating the weak water–rock interactions. The stable α -quartz would not interact with acid fluids (condensed fluid and/or spring water) from Zhenzhu Spring. Although the full evaporation of the condensed fluid from Zhenzhu Spring can form some amorphous silica (Fig. 5b) because the condensed fluid contains a small concentration of SiO₂ (Table 1), it is difficult to explain why amorphous silica appeared under the gypsum crystals (Fig. 4) and why there is a larger amount of amorphous silica than gypsum. Indeed, the condensed fluids contributed some silica to the amorphous silica deposits. Their contribution, however, was limited compared with that of the spring water. Thus, the spring water would be the main silica source of amorphous silica precipitates in the rock coatings from Zhenzhu Spring.

Amorphous silica precipitates in the rock coatings at Zhenzhu Spring are formed subaerially. Several processes were proposed to explain the formation of subaerial amorphous silica in hot springs: splashing, oscillatory changes in the water level (e.g. wave action), steam condensation and capillary action (Walter, 1976; Jones *et al.* 1997; Campbell *et al.* 2002; Mountain *et al.* 2003; Jones & Renaut, 2006). At Zhenzhu Spring, the splashing water cannot reach the areas where the rock coatings are formed. Moreover, dissolved SiO₂ cannot be supplied by oscillatory changes in the water level because of the stable pool water depth of Zhenzhu Spring. Accordingly, the capillary rise of the spring water, also termed wicking (Hinman & Lindstrom, 1996), would be necessary for the formation of subaerial amorphous silica in the rock coatings at Zhenzhu Spring. The spring water ascended to the lower part of the rock coatings at Zhenzhu Spring by capillary action

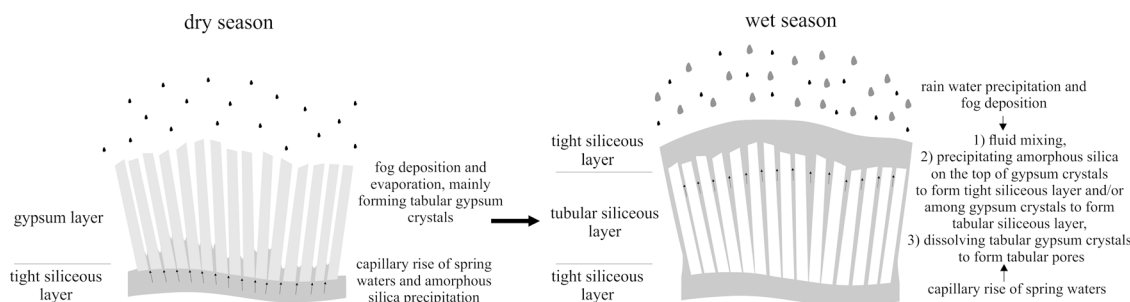


Fig. 6. Schematic diagrams showing the development of siliceous rock coatings in the dry season (a) and the wet season (b). The tabular gypsum crystals were mainly formed in the dry season, and the alternating siliceous layers were formed in the wet season.

(Fig. 6) and precipitated amorphous silica among gypsum crystals resulting from the evaporation and/or cooling of the spring water (Fig. 6c, d).

5.c. Laminae controlled by dissolution, capillary action and acid-fog deposition

Most of the rock coatings from Zhenzhu Spring are formed of multiple layers, including the gypsum layers present at the top of the rock coatings and the alternating siliceous layers developed below the gypsum layer (Fig. 4). As discussed above, the gypsum crystals are produced by acid-fog deposition and subsequent evaporation, and the siliceous minerals are the result of the capillary rise of the spring water and cooling/evaporation. The higher amorphous silica contents in the rock coatings and the alternation of siliceous layers are interesting. The former may be caused by (1) larger contribution of capillary spring waters to the rock coatings than contribution of fog, (2) dissolution of gypsum by the capillary waters or meteoric waters (Fig. 6), and (3) weak water–rock interactions between acid fluids and muscovite, which would leach a little SiO_2 (Fig. 5g). However, the alternation of siliceous layers is still unclear.

Laminated development has been found to be a common characteristic of hot spring deposits in Tengchong (e.g. Jones & Peng, 2012, 2015). Konhauser *et al.* (2001) suggested that seasonal climate change is responsible for the development of the cyclic siliceous laminae. Intrinsic control (aperiodic CO_2 content changes in the spring water) was also proposed to interpret the development of the tripartite growth cycle in travertines (Jones & Peng, 2012, 2014). However, these hot spring deposits are all considered to be formed subaqueously, unlike the subaerial siliceous-sulphate coatings at Zhenzhu Spring.

The subtropical monsoon climate in Tengchong causes significant variations in rainfall between the wet season and the dry season. Data from Jones & Peng (2015) show that c. 80 % of total rainfall is concentrated in the wet season (average 210 mm/month). This change accounts for the seasonal development of gypsum. In the dry season, the acid-fog deposition on the surface of rock coatings and subsequent complete evaporation led to the formation of gypsum crystals on the rock-coating surface (gypsum layer, Fig. 6). Continuous rain in the wet season diluted the condensed fluid and reduced the saturation level of the condensed water with respect to gypsum. Thus, little or no gypsum was precipitated on the rock-coating surface in the wet season.

Rainfall events can cause the dissolution of many metal sulphate minerals (Jambor *et al.* 2000). Although the spring waters of Zhenzhu Spring were unsaturated with gypsum (Fig. 5c), little gypsum was dissolved in the dry season because the capillary spring

waters might only arrive at the lower part of the rock coatings due to the low groundwater level (Fig. 6). In the wet season, the capillary waters might rise to the surface of the rock coatings and mix with the rainwater and some condensed fluids. This dilution process strengthened the gypsum-dissolving capacity of the diluted capillary waters. Thus, affected by perennial rains, the earlier-formed gypsum was dissolved by the capillary waters during the wet season and produced tabular pores (Fig. 6).

The changes in rainfall controlled the precipitation of amorphous silica in the rock coatings at Zhenzhu Spring. Although heavy rains would increase the groundwater level and drive the capillary waters to cover the rock-coating surfaces, they would dilute the capillary waters. Slight dilution of the capillary waters decreased the SI of amorphous silica (Fig. 5f), but amorphous silica would still be formed until it reaches undersaturation. Weak capillary action in the dry season explains the occurrence of amorphous silica in the lower part of gypsum crystals (Fig. 6). Abundant amorphous silica was formed in the wet season, when the diluted capillary water covered the surface of the rock coatings. However, it is must be emphasized that heavy rain events (high dilution factors) would prevent the formation of amorphous silica and accelerate the dissolution of gypsum. The amorphous silica precipitation would therefore cease after the strong dilution (dilution factor ≥ 1.35 , $T = 20^\circ\text{C}$) of the capillary waters (Fig. 5f).

Accordingly, the growth and development of the laminae of the rock coatings at Zhenzhu Spring involved the acid-fog deposition process, the capillary action of spring water, and the dissolution process influenced by the seasonal climate change (Fig. 6). The acid-fog deposition in the dry season and subsequent evaporation formed the gypsum layer at the top of the rock coatings. The capillary action of the spring waters supplied silica to the rock coatings, but this process was influenced by the seasonal climate change (especially rainfall variations). Amorphous silica was mainly precipitated among tabular gypsum crystals to form tabular aggregates and on the rock coating surface to form tight siliceous layers in the wet season, when there was still a small amount of rainwater. Heavy rains interrupted the precipitation of amorphous silica and enhanced the dissolution of gypsum crystals forming many tabular siliceous pores. Thus, the tight siliceous layers and the tabular siliceous layers were formed in the wet season. In the case of the siliceous debris layers, they largely originated from the breakage and/or dissolution of the tabular siliceous layers.


6. Conclusions

The rock coatings from Zhenzhu Spring are mainly composed of gypsum and amorphous silica along with some alum-(K), voltaite,

α -quartz and muscovite. The various laminations of the rock coatings found at Zhenzhu Spring can be divided into the following layers: gypsum, tight siliceous, tabular siliceous and siliceous debris. The siliceous debris layers might be the products of the breakage (and dissolution) of the tabular siliceous layers, possibly resulting from rainfall events in the wet season. Both the spring waters and the condensed fluids are rich in SO_4^{2-} . Large differences in concentrations of other ions and SiO_2 are, however, evident between the spring waters and the condensed fluids. Geochemical models indicate that the formation of gypsum is closely linked to the condensed fluids, while the precipitation of amorphous silica is mainly influenced by the cooling and/or evaporation of the capillary spring waters.

This study shows that the rock coatings are the integrated product of acid-fog deposition, capillary action of spring water, and dissolution. The acid-fog deposition (and cooling/condensation) produced water films and droplets on the rock surface. Gypsum only occurred after the complete evaporation of the condensed fluids in the dry season. Meanwhile, some spring waters were delivered to the lower part of the rock coatings by capillary action and precipitated amorphous silica. This capillary rise process became stronger with larger rainfall amounts in the wet season. Controlled by the variations in rainfall, the precipitation of amorphous silica was fluctuant. A small amount of rain caused the capillary spring waters supersaturated with amorphous silica to cover the rock-coating surface, forming a tight siliceous layer, and to fill the pores among tabular gypsum crystals, forming many tabular siliceous aggregates. Nevertheless, rainwater diluted the capillary waters and prevented the further formation of amorphous silica. Meanwhile, the diluted capillary water continuously dissolved the tabular gypsum crystals, forming a tabular siliceous layer or a siliceous debris layer. Thus, the alternating siliceous layers were all formed in the wet season.

The development of the siliceous-sulphate rock coatings suggests the effect of acid-fog deposition on subaerial sulphate minerals around hot springs. In most of the acid sulphate hot springs and similar environments, the effect of acid-fog deposition, however, might be masked by other processes (e.g. acid-sulphate alteration). The preservation of sulphate minerals formed by acid-fog deposition is difficult in wet conditions (e.g. rainfall events). This study also shows the significance of capillary action in the formation of subaerial amorphous silica in hot springs.

Author ORCIDs.  Huaguo Wen, 0000-0002-5140-1045

Acknowledgements. This research was financially supported by the National Natural Science Foundation of China (grant No. 41572097 to Wen). We thank the Yunnan Tengchong Rehai Tour Developing Co. Ltd for giving access to the Rehai geothermal field. We also thank Weirong Dai for help during field observation at Zhenzhu Spring. We are indebted to Rongcai Zheng who provides much technical assistance. Finally, we would like to thank the Editor Stephen Hubbard for his kindly assistance and the reviewers (Dr Alejandro Rodríguez and two anonymous reviewers) for their useful suggestions and comments on an earlier version of this work.

References

- Africano F and Bernard A** (2000) Acid alteration in the fumarolic environment of Usu volcano, Hokkaido, Japan. *Journal of Volcanology and Geothermal Research* **97**, 475–95.
- Aguilera F, Layana S, Rodríguez Díaz A, González C, Cortés J and Inostroza M** (2016) Hydrothermal alteration, fumarolic deposits and fluids from Lastarria Volcanic Complex: a multidisciplinary study. *Andean Geology* **43**, 166–96.
- Archontidou A, Blondé F and Picon M** (2005) Observations techniques et archéométriques sur l'atelier d'Apothika (Lesbos). In *L'Alun de Méditerranée* (eds P Borgard, J-P Brun and M Picon), pp. 89–96. Centre Jean Bérard, Naples, Aix-en-Provence: Colloque International, Naples, Lipari Juin.
- Bai DH, Meju MA and Liao ZJ** (2001) Magnetotelluric images of deep crustal structure of the Rehai geothermal field near Tengchong, southern China. *Geophysical Journal International* **147**, 677–87.
- Bogdan PO, Herta SE, Jonethan GW and Ioan P** (2013) Rapidcreekite in the sulfuric acid weathering environment of Diana Cave, Romania. *American Mineralogist* **98**, 1302–9.
- Campbell KA, Rodgers KA, Brotheridge JMA and Browne PRL** (2002) An unusual modern silica-carbonate sinter from Pavlova spring, Ngatamariki, New Zealand. *Sedimentology* **49**, 835–54.
- Ciesielczuk J, Zaba J, Bzowska G, Gaidzik K and Głogowska M** (2013) Sulphate efflorescences at the geyser near Pinchollo, southern Peru. *Journal of South American Earth Sciences* **42**, 186–93.
- Du J, Liu C, Fu B, Ninomiya Y, Zhang Y, Wang C, Wang H and Sun Z** (2005) Variations of geothermometry and chemical-isotopic compositions of hot spring fluids in the Rehai geothermal field, southwestern China. *Journal of Volcanology and Geothermal Research* **142**, 243–61.
- Guidry SA and Chafetz HS** (2002) Factors governing subaqueous siliceous sinter precipitation in hot springs: examples from Yellowstone National Park, USA. *Sedimentology* **49**, 1253–67.
- Guo Q, Liu M, Li J, Zhang X and Wang Y** (2014) Acid hot springs discharged from the Rehai hydrothermal system of the Tengchong volcanic area (China): formed via magmatic fluid absorption or geothermal steam heating? *Bulletin of Volcanology* **76**, 868–79.
- Guo Q and Wang Y** (2012) Geochemistry of hot springs in the Tengchong hydrothermal areas, Southwestern China. *Journal of Volcanology and Geothermal Research* **215–216**, 61–73.
- Guo QH** (2012) Hydrogeochemistry of high-temperature geothermal systems in China: a review. *Applied Geochemistry* **27**, 1887–98.
- Handley KM, Campbell KA, Mountain BW and Browne PRL** (2005) Abiotic controls on the origin and development of spicular sinter: in situ growth experiments, Champagne Pool, Waiotapu, New Zealand. *Geobiology* **3**, 93–114.
- Henderson JH, Syers JK and Jackson ML** (1970) Quartz dissolution as influenced by pH and the presence of a disturbed surface layer. *Israel Journal of Chemistry* **8**, 357–72.
- Herdianita NR, Rodgers KA and Browne PRL** (2000) Routine instrumental procedures to characterise the mineralogy of modern and ancient silica sinters. *Geothermics* **29**, 65–81.
- Hinman NW and Lindstrom RF** (1996) Seasonal changes in silica deposition in hot spring systems. *Chemical Geology* **132**, 237–46.
- Hynek BM, McCollom TM, Marcucci EC, Brugman K and Rogers KL** (2013) Assessment of environmental controls on acid-sulfate alteration at active volcanoes in Nicaragua: applications to relic hydrothermal systems on Mars. *Journal of Geophysical Research: Planets* **118**, 2083–104.
- Jackson ML** (1958) *Soil Chemical Analysis*. Englewood Cliffs, New Jersey: Prentice Hall, pp. 260–1.
- Jambor JL, Nordstrom DK and Alpers CN** (2000) Metal-sulfate salts from sulfide mineral oxidation. *Reviews in Mineralogy and Geochemistry* **40**, 303–50.
- Jiang Z, Li P, Tu J, Wei DZ, Zhang R, Wang YH and Dai XY** (2018) Arsenic in geothermal systems of Tengchong, China: potential contamination on freshwater resources. *International Biodeterioration & Biodegradation* **128**, 28–35.
- Jones B and Peng X** (2012) Intrinsic versus extrinsic controls on the development of calcite dendrite bushes, Shuzhishi Spring, Rehai geothermal area, Tengchong, Yunnan Province, China. *Sedimentary Geology* **249**, 45–62.
- Jones B and Peng X** (2014) Hot spring deposits on a cliff face: a case study from Jifei, Yunnan Province, China. *Sedimentary Geology* **302**, 1–28.
- Jones B and Peng X** (2015) Laminae development in opal-A precipitates associated with seasonal growth of the form-genus *Calothrix* (Cyanobacteria), Rehai geothermal area, Tengchong, Yunnan Province, China. *Sedimentary Geology* **319**, 52–68.

- Jones B and Renaut RW** (2006) Growth of siliceous spicules in acidic hot springs, Waiotapu geothermal area, North Island, New Zealand. *Palaiois* **21**, 406–23.
- Jones B, Renaut RW and Rosen MR** (1997) Biogenicity of silica precipitation around geysers and hot-spring vents, North Island, New Zealand. *Journal of Sedimentary Research* **67**, 88–104.
- Kavalieris I** (1994) High Au, Ag, Mo, Pb, V and W content of fumarolic deposits at Merapi volcano, central Java, Indonesia. *Journal of Geochemical Exploration* **50**, 479–91.
- Knauss KG and Wolery TJ** (1988) The dissolution kinetics of quartz as a function of pH and time at 70°C. *Geochimica et Cosmochimica Acta* **52**, 43–53.
- Kodosky L and Keskinen M** (1990) Fumarole distribution, morphology, and encrustation mineralogy associated with the 1986 eruptive deposits of mount St. Augustine, Alaska. *Bulletin of Volcanology* **52**, 175–85.
- Konhauser KO, Phoenix VR, Bottrell SH, Adams DG and Head IM** (2001) Microbial-silica interactions in Icelandic hot spring sinter: possible analogues for some Precambrian siliceous stromatolites. *Sedimentology* **48**, 415–33.
- Kruszewski Ł** (2013) Supergene sulphate minerals from the burning coal mining dumps in the Upper Silesian Coal Basin, South Poland. *International Journal of Coal Geology* **105**, 91–109.
- Leybourne MI, Cameron EM, Reich M, Palacios C, Faure K and Johannesson KH** (2013) Stable isotopic composition of soil calcite (O, C) and gypsum (S) overlying Cu deposits in the Atacama Desert, Chile: implications for mineral exploration, salt sources, and paleoenvironmental reconstruction. *Applied Geochemistry* **29**, 55–72.
- Lin MS, Peng SB, Qiao WT and Li H** (2014) Petro-geochemistry and geochronology of late Cretaceous–Eocene granites in high geothermal anomaly areas in the Tengchong block, Yunnan Province, China and their tectonic implications. *Acta Petrologica Sinica* **30**, 527–46 (in Chinese with English abstract).
- Luo L, Wen H, Li Y, You Y and Luo X** (2019a) Mineralogical, crystal morphological, and isotopic characteristics of smooth slope travertine deposits at Reshuitang, Tengchong, China. *Sedimentary Geology* **381**, 29–45.
- Luo L, Wen H, Zheng R, Liu R, Li Y, Luo X and You Y** (2019b) Subaerial sulfate mineral formation related to acid aerosol at Zhenzhu Spring, Tengchong, China. *Mineralogical Magazine*, 1–12. doi: [10.1180/mgm.2018.164](https://doi.org/10.1180/mgm.2018.164).
- Martin R, Rodgers K and Browne P** (2000) Aspects of the distribution and movement of aluminium in the surface of the Te Kopia geothermal field, Taupo Volcanic Zone, New Zealand. *Applied Geochemistry* **15**, 1121–36.
- McCanta MC, Dyar MD, Elkinstanton LT and Treiman AH** (2014) Alteration of Hawaiian basalts under sulfur-rich conditions: applications to understanding surface-atmosphere interactions on Mars and Venus. *American Mineralogist* **99**, 291–302.
- Minitti ME, Weitz CM, Lane MD and Bishop JL** (2007) Morphology, chemistry, and spectral properties of Hawaiian rock coatings and implications for Mars. *Journal of Geophysical Research: Planets* **112**, E05015. Doi: [10.1029/2006JE002839](https://doi.org/10.1029/2006JE002839).
- Mountain BW, Benning LG and Boerema JA** (2003) Experimental studies on New Zealand hot spring sinters: rates of growth and textural development. *Canadian Journal of Earth Sciences* **40**, 1643–67.
- Parkhurst DL and Appelo CAJ** (1999) *User's Guide to PHREEQC (Version 2): A Computer Program for Speciation, Batch-Reaction, One-Dimensional Transport, and Inverse Geochemical Calculations*. Boulder, Colorado: US Geological Survey. *Water-Resources Investigations Report* 99-4259.
- Peng X and Jones B** (2012) Rapid precipitation of silica (opal-A) disguises evidence of biogenicity in high-temperature geothermal deposits: case study from Dagunguo hot spring, China. *Sedimentary Geology* **257–260**, 45–62.
- Pierre D and Alain B** (1994) Geochemistry, mineralogy, and chemical modeling of the acid crater lake of Kawah Ijen Volcano, Indonesia. *Geochimica et Cosmochimica Acta* **58**, 2445–60.
- Piochi M, Mormone A, Balassone G, Strauss H, Troise C and De Natale G** (2015) Native sulfur, sulfates and sulfides from the active Campi Flegrei volcano (southern Italy): genetic environments and degassing dynamics revealed by mineralogy and isotope geochemistry. *Journal of Volcanology and Geothermal Research* **304**, 180–93.
- Renaut RW, Jones B and Tiercelin JJ** (1998) Rapid in situ silicification of microbes at Loburu hot springs, Lake Bogoria, Kenya Rift Valley. *Sedimentology* **45**, 1083–103.
- Rodgers KA, Browne PRL, Buddle TF, Cook KL, Greatrex RA, Hampton WA, Herdianita NR, Holland GR, Lynne BY, Martin R, Newton Z, Pastars D, Sannazarro KL and Teece CIA** (2004) Silica phases in sinters and residues from geothermal fields of New Zealand. *Earth-Science Reviews* **66**, 1–61.
- Rodgers KA, Cook KL, Browne PRL and Campbell KA** (2002) The mineralogy, texture and significance of silica derived from alteration by steam condensate in three New Zealand geothermal fields. *Clay Minerals* **37**, 299–322.
- Rodgers KA, Hamlin KA, Browne PRL, Campbell KA and Martin R** (2000) The steam condensate alteration mineralogy of Ruatapu cave, Orakei Korako geothermal field, Taupo Volcanic Zone, New Zealand. *Mineralogical Magazine* **64**, 125–42.
- Rodríguez A and van Bergen MJ** (2016) Volcanic hydrothermal systems as potential analogues of Martian sulphate-rich terrains. *Netherlands Journal of Geosciences* **95**, 153–69.
- Rodríguez A and van Bergen MJ** (2017) Superficial alteration mineralogy in active volcanic systems: an example of Poás volcano, Costa Rica. *Journal of Volcanology and Geothermal Research* **346**, 54–80.
- Schiffman P, Zierenberg R, Marks N, Bishop JL and Dyar MD** (2006) Acid-fog deposition at Kilauea volcano: a possible mechanism for the formation of siliceous-sulfate rock coatings on Mars. *Geology* **34**, 921–24.
- Settle M** (1979) Formation and deposition of volcanic sulfate aerosols on Mars. *Journal of Geophysical Research: Solid Earth* **84**, 8343–54.
- Shangguan Z** (2000) Structure of geothermal reservoirs and the temperature of mantle-derived magma hot source in the Rehai area, Tengchong. *Acta Petrologica Sinica* **16**, 83–90 (in Chinese with English abstract).
- Shangguan Z, Bai C and Sun M** (2000) Mantle-derived magmatic gas releasing features at the Rehai area, Tengchong county, Yunnan Province, China. *Science in China Series D – Earth Sciences* **43**, 132–40.
- Shangguan Z, Zhao C, Li H, Gao Q and Sun M** (2005) Evolution of hydrothermal explosions at Rehai geothermal field, Tengchong volcanic region, China. *Geothermics* **34**, 518–26.
- Shimobayashi N, Ohnishi M and Miura H** (2011) Ammonium sulfate minerals from Mikasa, Hokkaido, Japan: boussingaultite, godovikovite, efremovite and tschermigite. *Journal of Mineralogical and Petrological Sciences* **106**, 158–63.
- Singer CJ** (1948) *The Earliest Chemical Industry: An Essay in the Historical Relations of Economics and Technology Illustrated from the Alum Trade*. London: Folio Society, 52 pp.
- Szynkiewicz A, Borrok DM and Vaniman DT** (2014) Efflorescence as a source of hydrated sulfate minerals in valley settings on Mars. *Earth and Planetary Science Letters* **393**, 14–25.
- Tang M, Ehreiser A and Li YL** (2014) Gypsum in modern Kamchatka volcanic hot springs and the Lower Cambrian black shale: applied to the microbial-mediated precipitation of sulfates on Mars. *American Mineralogist* **99**, 2126–37.
- Taran YA, Bernard A, Gavilanes JC, Lunezheva E, Cortés A and Armienta MA** (2001) Chemistry and mineralogy of high-temperature gas discharges from Colima volcano, Mexico. Implications for magmatic gas–atmosphere interaction. *Journal of Volcanology and Geothermal Research* **108**, 245–64.
- Tobler DJ, Stefansson A and Benning LG** (2008) In-situ grown silica sinters in Icelandic geothermal areas. *Geobiology* **6**, 481–502.
- Tosca NJ, McLennan SM, Lindsley DH and Schoonen MAA** (2004) Acid-sulfate weathering of synthetic Martian basalt: the acid fog model revisited. *Journal of Geophysical Research: Planets* **109**, E05003. doi: [10.1029/2003JE002218](https://doi.org/10.1029/2003JE002218).
- Valente TM and Gomes CL** (2009) Occurrence, properties and pollution potential of environmental minerals in acid mine drainage. *Science of the Total Environment* **407**, 1135–52.
- Walter MR** (1976) Geysers of Yellowstone National Park: an example of abiogenic “stromatolites”. In *Developments in Sedimentology* (ed. MR Walter), pp. 87–112. Amsterdam: Elsevier.

- Yant M, Young KE, Rogers AD, McAdam AC, Bleacher JE, Bishop JL and Mertzman SA** (2018) Visible, near-infrared, and mid-infrared spectral characterization of Hawaiian fumarolic alteration near Kilauea's December 1974 flow: implications for spectral discrimination of alteration environments on Mars. *American Mineralogist* **103**, 11–25.
- Zhang GP, Liu CQ, Liu H, Jin ZS, Han GL and Li L** (2008) Geochemistry of the Rehai and Ruidian geothermal waters, Yunnan Province, China. *Geothermics* **37**, 73–83.
- Zhang M, Guo Z, Sano Y, Zhang L, Sun Y, Cheng Z and Yang TF** (2016a) Magma-derived CO₂ emissions in the Tengchong volcanic field, SE Tibet: implications for deep carbon cycle at intra-continent subduction zone. *Journal of Asian Earth Sciences* **127**, 76–90.
- Zhang Y, Tan H, Zhang W, Wei H and Dong T** (2016b) Geochemical constraint on origin and evolution of solutes in geothermal springs in western Yunnan, China. *Chemie der Erde – Geochemistry* **76**, 63–75.
- Zhao C, Ran H and Chen K** (2011) Present-day temperatures of magma chambers in the crust beneath Tengchong volcanic field, southwestern China: estimation from carbon isotopic fractionation between CO₂ and CH₄ of free gases escaped from thermal springs. *Acta Petrologica Sinica* **27**, 2883–97 (in Chinese with English abstract).
- Zhu MX, Tong W and You MZ** (1982) Efflorescence in geothermal areas of Xizang (Tibet) and its geological significance. *Acta Scientiarum Naturalium Universitatis Pekinesis* **18**, 110–17 (in Chinese with English abstract).